Polytetrafluoroethylene Sputtered PES Membranes for Membrane Distillation: Influence of RF Magnetron Sputtering Conditions

Sara Pedram, Hamid R. Mortaheb, Houssam Fakhouri, Farzaneh Arefi-Khonsari

Polytetrafluoroethylene sputtered PES membranes for membrane distillation: Influence of RF magnetron sputtering conditions

Sara Pedram[1, 2], Hamid R. Mortaheb[1,*], Houssam Fakhouri[2], Farzaneh Arefi-Khonsari[2]

[1] Oil Engineering Department, Chemistry and Chemical Engineering Research Center of Iran, PO Box 14335-186, Tehran, Iran

[2] Sorbonne Universités, UPMC Univ Paris 6, UMR8235, LISE, 4 Place Jussieu, 75252 Paris, France

Abstract

Thin films of fluorocarbon were deposited on polyethersulfone membranes via argon plasma sputtering of a poly (tetrafluoroethylene) (PTFE) target in an RF magnetron plasma reactor. The obtained deposited ultrathin coatings had nanoscale roughnesses and high degrees of fluorination. The intensity of fluorine atom in plasma environment during fluorocarbon deposition was investigated. Depending on the deposition conditions comprising working gas pressure, applied RF power, and distance between the target and the substrate, polymeric films with different chemical compositions and/or morphologies were obtained. The morphologies of the films were analyzed by means of SEM, XPS, and AFM. The results suggested that the sputtered film deposited at a higher pressure and longer target-substrate distance and moderate RF power had a surface composition and chemical structure closer to those of the PTFE film. The treated hydrophobic PES membranes with water contact angles as high as 115° were applied for the first

* Corresponding author.
email: mortaheb@ccerci.ac.ir (H. R. Mortaheb), Tel. +98 21 44787751; Fax: +98 21 44787781.

time in an air gap membrane distillation (AGMD) setup for removal of benzene as a volatile organic compound from water. The results showed that the plasma-treated membranes have a comparable or superior performance to that of commercial PTFE used in membrane distillation with similar permeate flux and separation factor after 20 h long term performance.

Keywords

PVD, Polytetrafluoroethylene (PTFE), RF magnetron sputtering, Thin film, Air gap membrane distillation, VOC removal.

1. Introduction

Membrane distillation (MD) is a thermally driven process whereby the volatile component from a feed solution is transmitted through a hydrophobic porous membrane and condensed on the other side. The membrane in the MD process reacts as a liquid/vapor interface and physical barrier between the hot feed side and the distillate side [1, 2].

The most important requirement for a MD process relies on the usage of a non-wetting membrane to prevent the entry of liquid into the membrane pores. During the process, a heated aqueous solution is brought into contact with one side of the membrane; a vapor liquid interface is formed at the pore inlet, and the liquid vaporizes at the pore inlet. Due to hydrophobic nature of the membrane, only transportation of the vapor through the membrane pores is allowed. The difference in vapor partial pressures is known as the driving force of the process. According to the procedure for vapor condensation/removal at the permeate side of the membrane, four configurations of Direct Contact Membrane Distillation (DCMD); Air Gap Membrane Distillation (AGMD); Sweeping Gas Membrane Distillation (SGMD); and Vacuum Membrane Distillation

(VMD) are defined for this process [3, 4]. Removal of volatile organic compounds (VOCs) from water is considered as an important application of the MD processes in water purification [5].

The surface chemistry, porosity, and pore size of the membrane have major roles in the process performance. An acceptable MD membrane should exhibit high water liquid entry pressure (LEP, defined as the minimum hydrostatic pressure, in which the liquid penetrates into the largest pores of a hydrophobic membrane), reasonable permeability, and high selectivity. The high surface porosity and pore size leads to high permeate flux though a high LEP is a result of small pores on the membrane surface [6, 7]. Therefore, attentions should be devoted for modification of membrane surface to obtain desirable separation performances.

Most of the applied MD membranes are based on polypropylene (PP), polyethylene (PE), polytetrafluoroethylene (PTFE), or polyvinylidene fluoride (PVDF), which are initially fabricated and designed for other applications [3, 5]. In some studies, commercially available hydrophobic membranes are post-treated for the MD process [8, 9].

Polyethersulfone is a polymer with excellent thermal stability, chemical inertness, and mechanical strength, which is commonly used for microfiltration, ultrafiltration, and gas separation processes [10–15]. It can be processed into membrane by a simple fabrication procedure (phase inversion method). The durability and low-price of this material encourage its application in the membrane processes. However, the presence of ether bonds in the membrane structure and therefore its partial hydrophilic characteristics limit the usage of this membrane in membrane distillation [16]. Therefore, some surface treatments are required to enhance the hydrophobicity of the PES membrane.

The hydrophobicity of a membrane for MD process can be obtained by altering the chemical composition of membrane surface. One of the lowest surface energy belongs to -CF_x groups which

make the fluorocarbon polymers the most favorable materials for fabrication of hydrophobic surfaces [17]. The investigations on hydrophobic properties of polytetrafluoroethylene (PTFE) thin films deposited by various methods i.e. chemical vapor deposition (CVD) [18] and physical vapor deposition (PVD) [19, 20] have been reported. Most of the methods particularly those, which are based on chemical syntheses, are complex or time-consuming or may release environmentally harmful substances [21]. In addition, processing of the conventional PTFE films and powders are difficult due to their chemical inertness and high crystallinity. A number of studies have been then performed to prepare PTFE-like thin films on different substrates using gas phase processing techniques [22].

One of the impressive techniques for fluoropolymer thin films preparation is radio frequency (RF) plasma sputtering of a PTFE target, first reported in the 1970s [23, 24] . Fluropolymer films deposited using plasma sputtering system have shown many advantageous such as high thermal stability, low dynamic friction coefficient, chemical inertness, low dielectric constant, bio-compatibility, and high hydrophobicity [22, 25].

In order to control the deposition mechanism and the subsequent polymer structure and to increase the hydrophobicity of the surface, parameters including process pressure, flow rate, carrier gas type, power, treatment time, and reactor geometry have been studied mostly focused on flat sheet surfaces such as silicon wafers [22], aluminum [26], and glass [27]. For examples, Zhang et al. [22] studied the effect of sputtering gas using Ar, CF_4, H_2, N_2, and O_2 on the dielectric constant and chemical composition and molecular structure of the sputter-deposited polymer films from a PTFE target. The CF_4 plasma had the highest fluorine content while H_2 plasma gave rise to a polyethylene-like film with very low fluorine content and the O_2 plasma gave no deposition on the surface. The dielectric constants of the deposited polymer film were increased in the following order by changing the type of the gas: $CF_4 < Ar < N_2 < H_2$.

Stelmashuk et al. [28] could represent that the static contact angle and fluorine concentration of the deposited films with RF sputtering of PTFE are increased as the argon pressure augmented up to 70 Pa. Despite the fact that long substrate-target distances in combination with high deposition pressures (20–100 Pa) in RF sputtering lead to low deposition rates, Drabik et al. [29] found that at pressures higher than 40 Pa and for the target–substrate distance longer than 25 cm, fluorocarbon plasma polymers similar to the structure and chemical composition of conventional PTFE could be deposited. Later, Kylian et al [25] reported that under elevated pressure and longer target-substrate distances, the deposited fluorocarbon polymer by means of RF magnetron sputtering of PTFE target in argon is composed of longer fluorocarbon chains. In another study, Suzuki et al. [30] found that crosslinking in the deposited fluorocarbon films and correspondingly its adhesion strength to the Si substrate are enhanced by increasing the substrate temperature in the range of -5 to 200°C. The flat sheet polypropylene (PP) membranes sputtered by PTFE in a RF plasma could represent absorption performance comparable to PTEF membranes for CO_2 separation in membrane gas absorption [31].

The present study deals with the treatment of hydrophilic-based PES membranes by PTFE plasma sputtering for applying in membrane distillation. The research aims to understand the influences of RF power, gas pressure, and target-substrate distance on the properties of the plasma and deposited polymer. The PTFE plasmas generated in an Ar atmosphere are studied using the optical emission spectroscopy (OES) technique. The surface treatment effects are characterized by means of Scanning Electron Microscopy (SEM), X-ray Photoelectron Spectroscopy (XPS), Atomic Force Microscopy (AFM), and static water contact angle (CA). The performances of treated membranes for removal of benzene from water are then evaluated in an air gap membrane distillation setup.

2. Experimental

Hydrophilic polyethersulfone granules (Ultrason E6020, Mw=58,000) were supplied from BASF. The flat sheet PES membranes were prepared by phase inversion technique as described in our previous study [32].

PTFE Sputtering is performed using the experimental set-up schematically depicted in Fig. 1. It consists of a cylindrical magnetron sputtering plasma reactor operated at a frequency of 13.56 MHz RF (SPT 120, Plasmionique, Canada) using a balanced magnetron cathode (MAGNION-B). The pumping system includes a turbo molecular pump (300 l/s, Varian TV301 Navigator) and a mechanical pump (ULVAC) for backing the turbo. The background pressure for all depositions is about $P_{b.g.} = 5\times10^{-6}$ Torr (6.7×10^{-4} Pa) while the total working pressure is adjusted between 3 to 20 mTorr (0.3 to 3 Pa). A PTFE disk (2-inch diameter) is used as the sputtering target for deposition of all films in an argon gas atmosphere. The RF power delivered by the generator is in the range of 15 to 100 W. The distance between substrate holder and the target is adjustable between 3-15 mm.

The plasma is characterized by optical emission spectroscopy (OES) using mono channel spectrometer (SpectraPro-500i, Action Research Corporation) with 0.500-meter triple grating monochromator/spectrograph and CD detector. Peak intensities of PTFE emission lines are normalized by that of mostly suggested at 811 nm Ar peak [33].

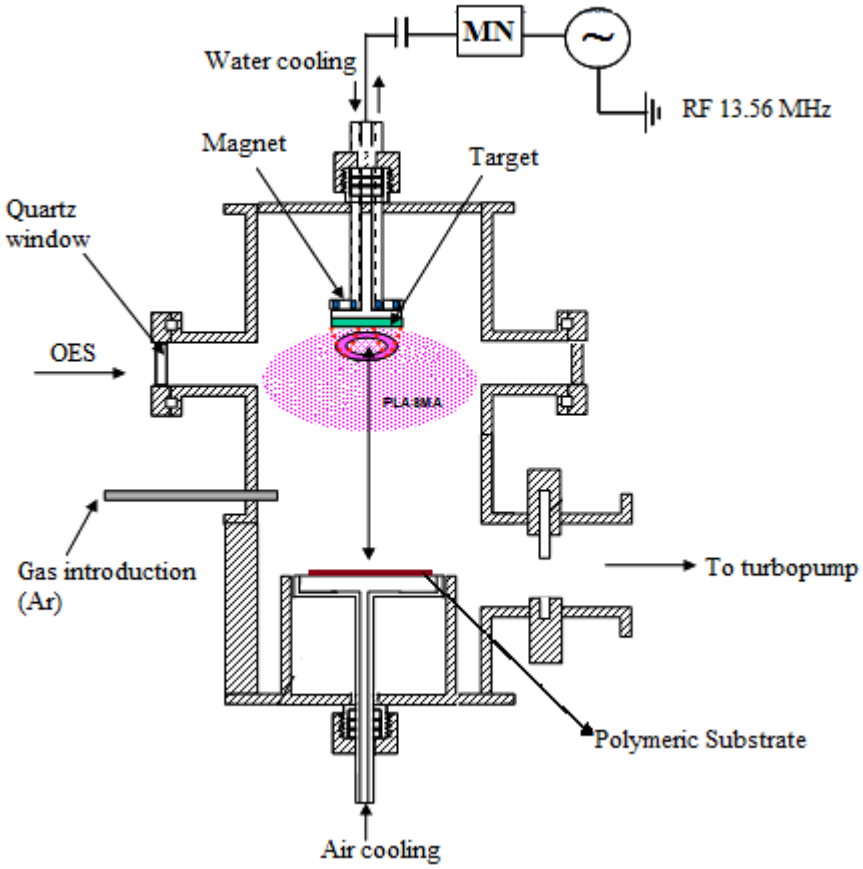

Fig. 1 schematic representation of RF magnetron sputtering experimental set-up.

The dynamic and static water contact angles of each prepared membrane are determined by sessile droplet method using contact angle goniometer (OCA 20, Data physics, Germany) at room temperature. And the average value obtained from five different spots is reported.

The liquid entry pressure (LEP) as an index of pore wetting behavior of the membrane is measured using an apparatus described elsewhere [34]. LEP is correlated with the interfacial tension, the contact angle at the pore entrance, and the size and shape of the membrane pores.

The surface porosity (ε_s) defined as the ratio between the pore areas to total surface area of the membrane, is a significant factor controlling the permeability and separation factor of MD membranes [5]:

$$\varepsilon_s = \frac{N\pi}{4}\sum_{j=1}^{n} f_j d_j^2 \quad (1)$$

where N is the number of pores per unit area, known also as the surface pore density, and f_j is the fraction of pores with size of d_j, which can be determined by AFM software program (DME-SPM 2.1.1.2) as described by Khayet [35].

The membrane volume porosity (ε) is obtained experimentally using a gravimetric method [36] and isooctane as the wetting liquid from the following equation:

$$\varepsilon = \frac{w_1 - w_2}{A \times l \times D} \quad (2)$$

where w_1 and w_2 , A, l, and D, are the weights of the wet and dry membranes, membrane effective area (cm^2), membrane thickness (cm), and isooctane density (D=0.69 g/cm^3), respectively.

The chemical compositions of PTFE coatings are investigated by an Omicron (ESCA+) X-ray photoelectron spectrometer equipped with a monochromatic aluminium K_α X-rays source ($h\nu$=1486.6 eV).

The topography of the deposited samples is studied by scanning electron microscopy (SEM) applying VEGA3-LM (Tescan). The samples are prepared by cryogenic breaking of the membrane followed by deposition of a thin gold layer. The surface morphology and roughness of the sputtered films are studied by AFM using DME Dual scope DS95-50-5E. In each case, an area of 5×5 μm^2 is scanned using the tapping mode at ambient pressure and room temperature.

The MD performances i.e. permeate fluxes and separation factors of the treated PES membranes are determined in a lab-scale AGMD set-up. The feed is a solution of 300 ppm benzene in water circulating with a flow rate of 3 ml/s. The feed and cooling water temperatures are set at 50 and 10°C, respectively. The permeated flux is determined by the weight of collected permeate from the experimental module during a 4-h run. The experimental set-up is shown in Fig. 2.

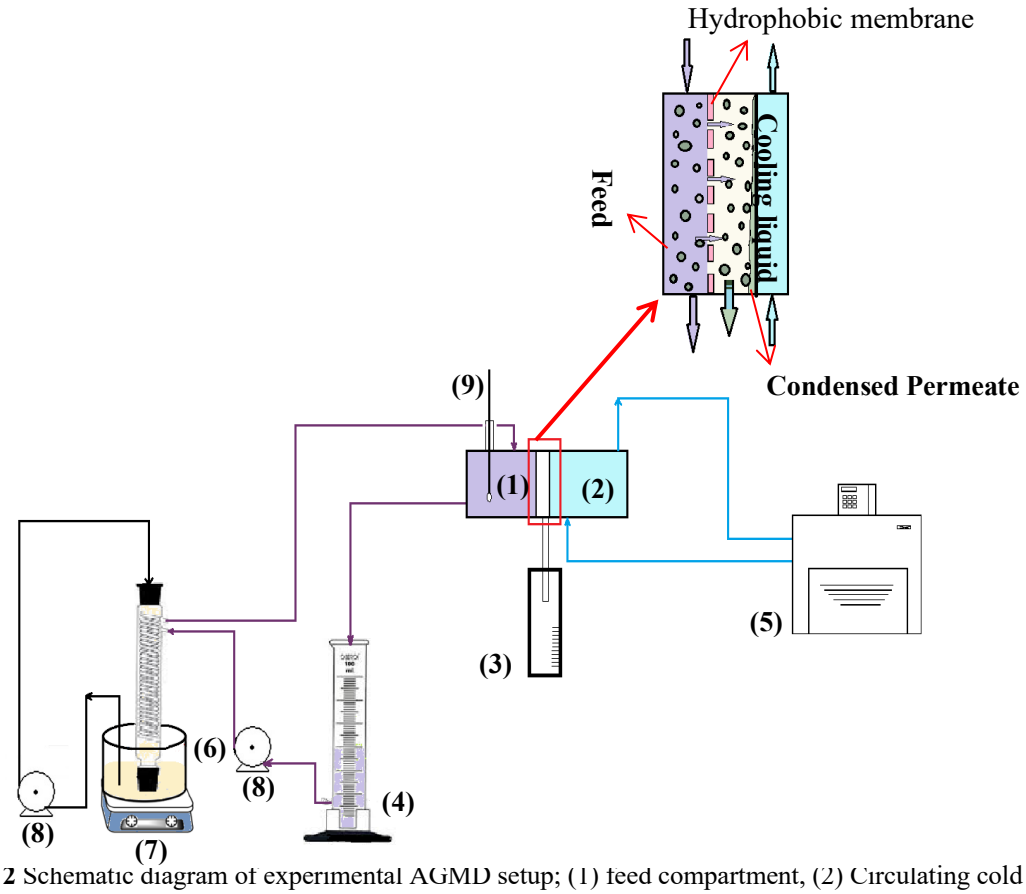

Fig. 2 Schematic diagram of experimental AGMD setup; (1) feed compartment, (2) Circulating cold water, (3) permeate collecting vessel, (4) feed vessel, (5) Cold circulator bath, (6) Paraffin bath, (7) heater, (8) pumps, (9) thermometer.

The separation factor of benzene is determined using the following equation:

$$\beta = \frac{y_B/(1-y_B)}{x_B/(1-x_B)} = \frac{y_B/x_B}{(1-y_B)/(1-x_B)} \quad (3)$$

where y_B and x_B represent the mole fractions of benzene in permeate and in the feed, respectively. The benzene concentration is determined by absorption UV–Vis spectroscopy (Perkin-Elmer Lambda 15 UV/VIS spectrophotometer) using the calibration curve.

3. Result and discussion

3.1. Optical emission spectroscopy

The optical fiber for the OES measurement is positioned behind the quartz viewing window as shown schematically in Fig. 1. Besides the lines of argon, used as the working gas, different spectral bands and lines are detected originating from the sputtering process. In this study, the lines correspond to argon neutrals Ar I (811 nm) and F neutrals F I (640, 677, 685 and 703 nm) [25, 37, 38] are followed. The F ions spectral lines are too weak to be detected properly and are not investigated. Fig. 3 shows the variation of different normalized fluorine lines in argon plasma as a function of power at the fixed argon pressure and flow rate. As shown in the figure, the most intense fluorine line measured by the SpectroPro-500i is the line at 705 nm. This result is consistent with the result of Canal et al. [38] where the F/Ar plasma in magnetron sputtering reactor was characterized. It is seen that increasing the power at fixed pressure can increase the normalized emission of F. As the power is increased, the plasma density is increased and thus the intensity of excited fluorine atoms is increased accordingly.

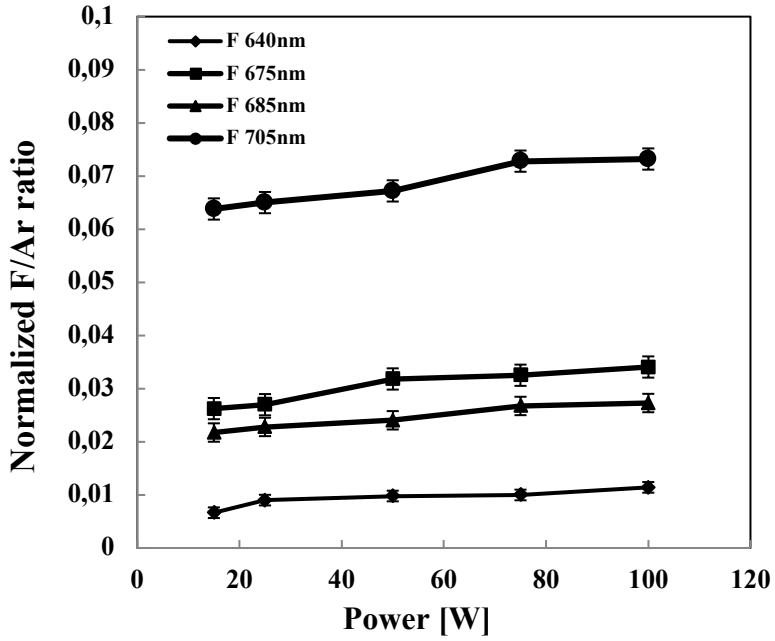

Fig. 3 Normalized emission intensities vs power at 3.5 mtorr (Q_{Ar} = 30 sccm).

Fig. 4 shows the OES intensities, and the normalized ones as a function of pressure, at low (50W) and high (100W) powers with Q_{Ar} = 30 sccm. It is found that the intensities of spectral peaks do not follow the same trend at these two powers. This behavior can be ascribed to the sputtering rate that is determined by the ion flux and ion energy distribution at the target. At the lower power (50 W) the sputtering rate decreases by increasing the pressure because the Ar ions lose their energies due to the increased collisions. At the higher power (100 W), the emission intensities increase at higher pressures by increasing the pressure even though the sputtering rate decreases. This is due to increased collisions of the energetic species. It means that a higher power accompanied with a higher pressure lead to a higher electron density and collision probability, and therefore a higher intensity of sputtered fluorine atoms is yielded.

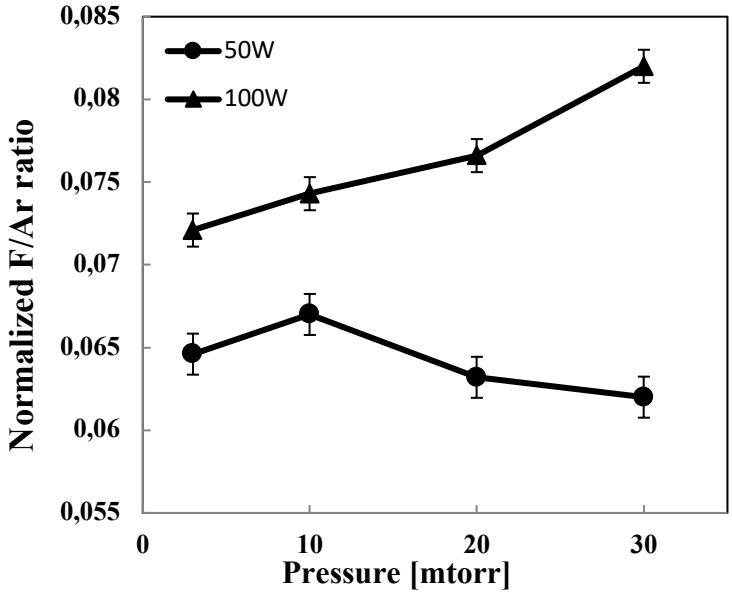

Fig. 4 Normalized emission intensities vs pressure (Q_{Ar}= 30sccm).

3.2. Characterization of fluorocarbon plasma polymer films

The changes in the plasma composition affect the chemical and physical properties of the deposited fluorocarbon films. The changes in the surface morphology are shown in Fig. 5 by means of SEM and AFM scans. The samples had comparable thicknesses of about 40 nm, which were measured by using a Quartz Crystal Microbalance (QCM) located next to the substrate holder in the sputtering chamber. The coating thickness was confirmed by measuring the thickness of sputtered coating on a silicon substrate in the SEM images. The samples were prepared at two different powers (50 W and 100 W), two different pressures (3.8 mtorr and 10 mtorr), and two different target-substrate distances (10 cm and 5 cm). The first row in Fig. 5 (a) shows the roughness of the deposited films for a target-substrate distance of 5 cm while the second row (b), shows a target-substrate distance of 10 cm. It can be seen in Fig. 5a that the roughness represented by the arithmetic average (S_a) is increased from 12.7 nm for the sample prepared at the low pressure (3.8mtorr) up to 21.7 nm for the sample prepared at the higher pressure(10mtorr) and 24.2 nm for higher power(100W), which is in agreement with the results of previous studies [25,

39, 40]. Indeed, it is well known that the mean momentum of the ions impinging the target and then the number of reactive ejected fragments from the target that reach and bombard the substrate are increased by increasing the RF power. The different chemical compositions of the created fragments and their energies result in formation of a highly crosslinked polymer, which will agglomerate on the surface and accounts for a high surface roughness [41]. The increase in the surface roughness of the deposited films with the pressure in the reactor can be explained considering the ion and energy fluxes reaching to the substrate. The higher sputtering pressures result in decrease of the mean free path and ionization probability with an increase in the number of collisions leading to a smaller kinetic energy of the sputtered species. The lower kinetic energy of the species bombarding the surface will lead to a lower surface mobility and therefore to formation of a 3D island growth (Volmer-Weber type of Growth which refers to the conditions, in which the atoms constituting the film have more interaction with themselves rather than to couple with the substrate. The three-dimensional islands are then nucleated and grown perpendicularly on the surface of the substrate.) [42–44]. It also causes a less crosslinked and more linear structure of the deposited coating. The lower target-substrate distance at fixed pressure results in the bombardment of the substrate with the sputtered species with a higher kinetic energy and therefore a higher surface mobility giving rise to a smoother deposited polymer.

(a)

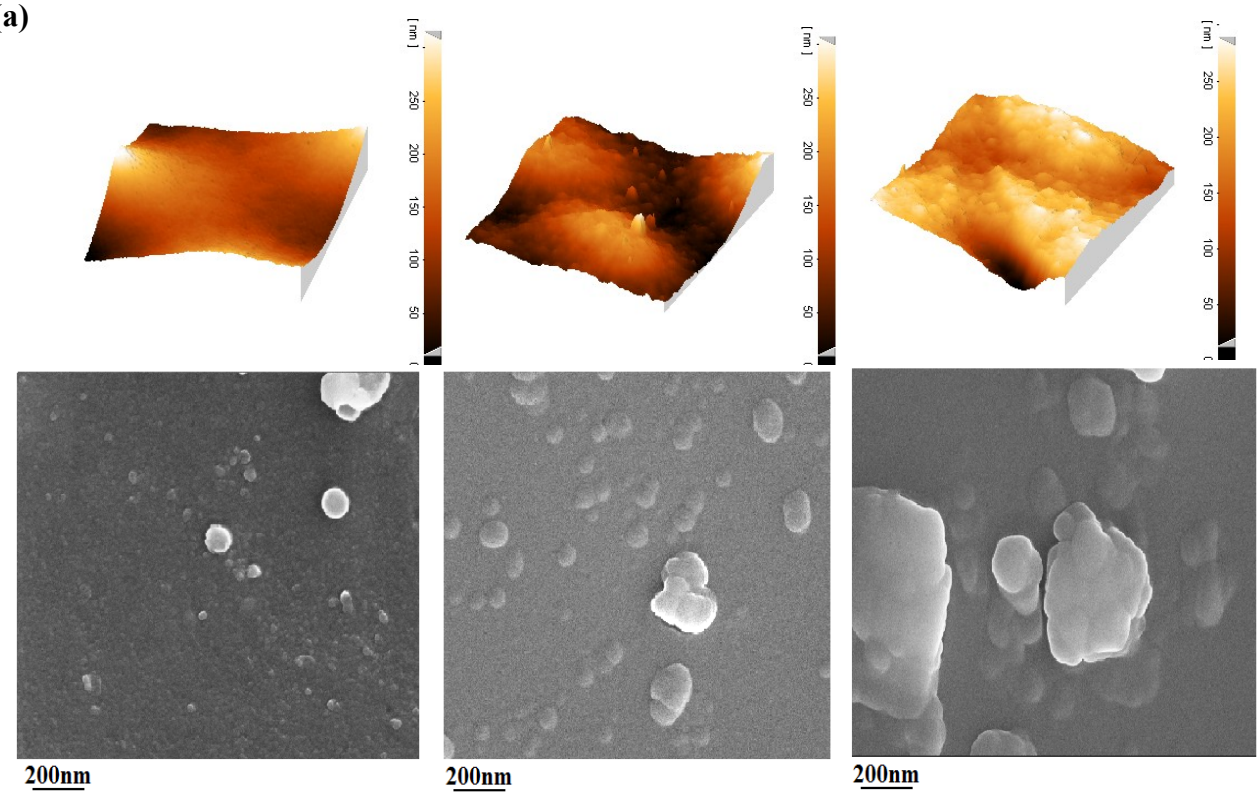

Power = 50 W, P=3.8 mtorr | Power = 50W, P=10 mtorr | Power = 100 W, P=3.8 mtorr

(b)

S_a= 12.7 nm | S_a= 21.7 nm | S_a= 24.2 nm

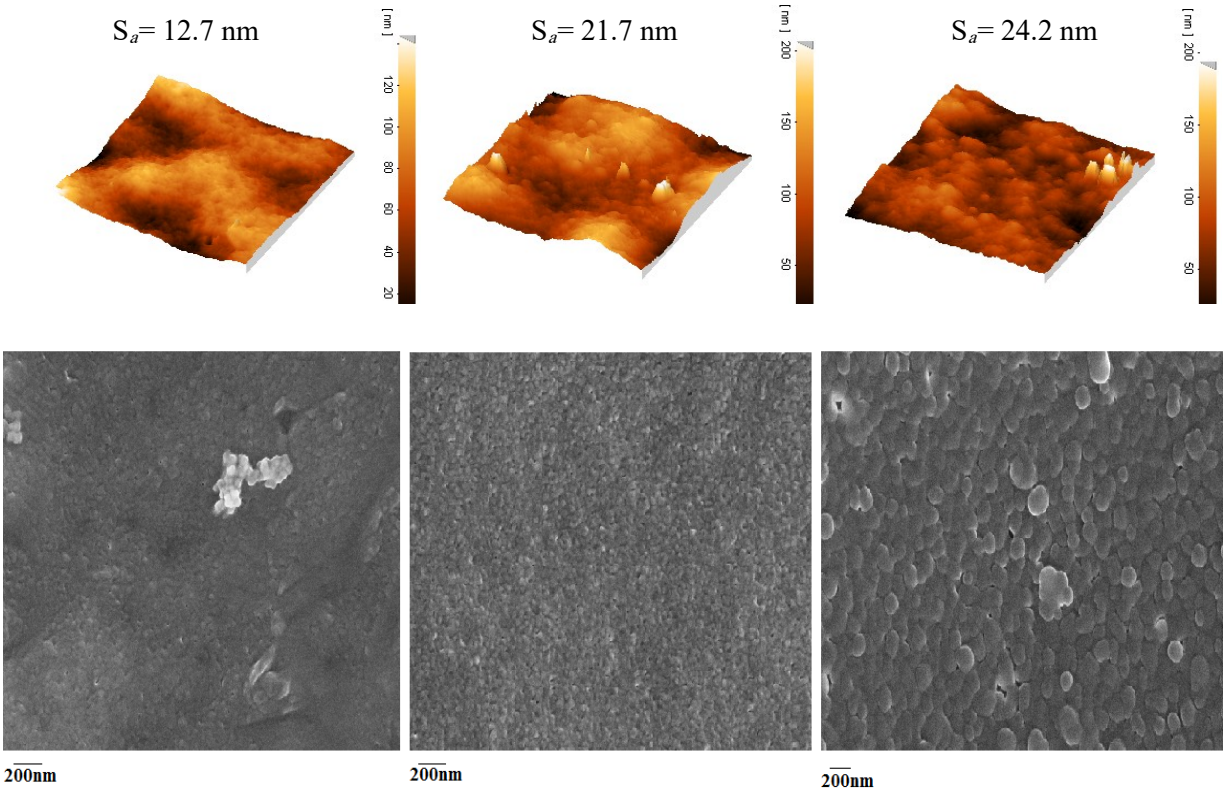

Power = 50 W, P=3.8 mtorr | Power = 50 W, P= 10 mtorr | Power = 100 W, P=3.8 mtorr

S_a= 15.4 nm | S_a= 25.2 nm | S_a= 28.1 nm

Fig. 5 AFM (bottom) and SEM (top) scans of fluorocarbon plasma polymer films deposited at different pressures and powers at sputtered target-substrate distances of **(a)** 5 cm and **(b)** 10 cm.

The compositions and chemical structures of the PTFE deposited films were investigated by XPS analysis. The high-resolution XPS scans of C1s peak containing peaks with chemical shifts due to C-C, –C-CF, -CF, -CF_2, and -CF_3 bonding [26–28] are given in Fig. 6. The fluorine abundance at the surface, [F]/[C] ratio calculated based on F and C atomic percentage reported by XPS, as an index parameter for determining the wettability of the surface was considered to determine the effect of sputtering parameters on the samples' surface chemistry [45–47]. The fractions of different CF_x chemical groups at different sputtering conditions as well as their [F]/[C] ratio are shown in Table 1.

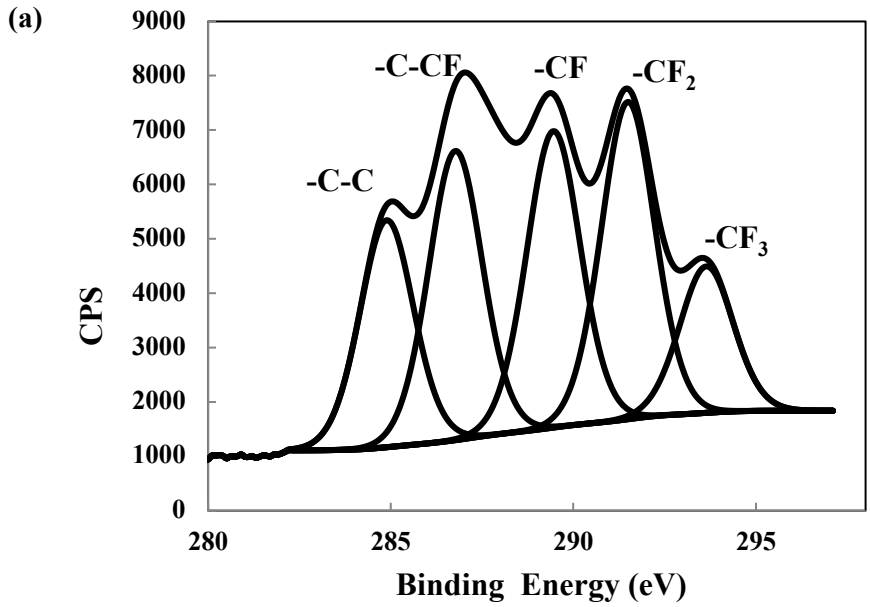

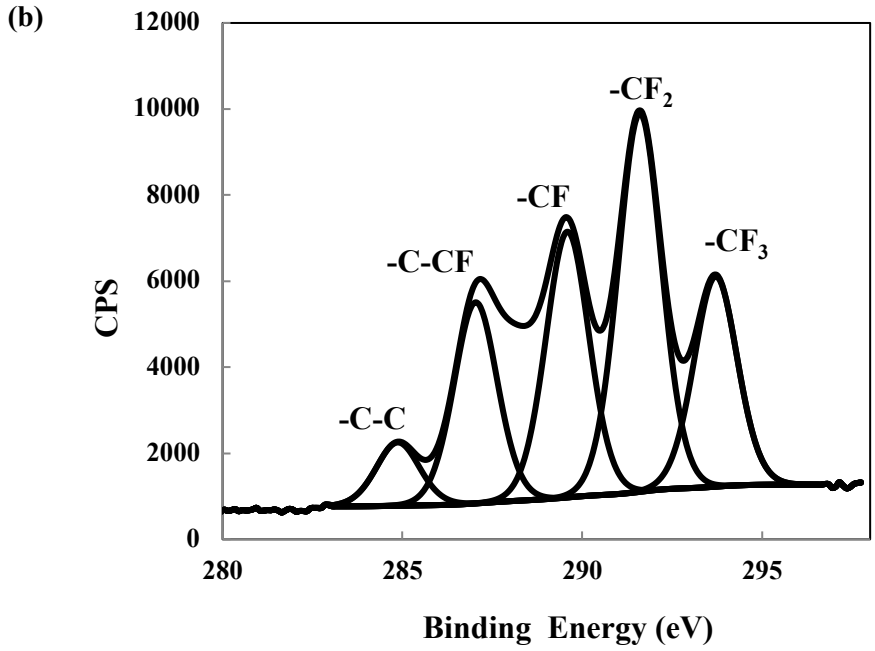

Fig. 6 XPS C1s core level of 10 min PTFE sputtering in Ar at **(a)** 50W, 3.4mtorr and 5 cm distance, and **(b)** 100W, 20 mtorr and 10 cm distance.

XPS spectra show that the chemical structure of the films changes with the PTFE sputtering conditions. Considering data reported in Table 1, in which the effect of each parameter can be evaluated by comparing two rows with different value of the tracked parameter at fixed two other parameters, the coatings prepared at higher pressures or target-substrate distances exhibit higher values of [F]/[C] ratio. In addition, a pronounced decrease in [F]/[C] was observed at higher powers. Lower [F]/[C] indicates that the coating consists of highly crosslinked-unsaturated structures [20, 25, 47]. At constant pressure, increasing the power results in an increase in the mean kinetic energy of the ions bombarding the target and thus increases the fragmentation of the polymeric target and consequently the kinetic energy of the fragments bombarding the substrate surface. Since the formation of unsaturated crosslinked components requires higher momentum transfer level supplied by the high-energy ions, the proportion of the crosslinked molecules will be increased by increasing the power [48]. Despite the fact that normalized F/Ar ratio, measured by OES, is increased by increasing the power, [F]/[C] ratio has a decreasing trend. This could be

due to enhancing the surface ablation resulting from the bombardment of the growing film on the substrate. On the other hand, increasing pressure or target-substrate distance tends to reduce the energy of the plasma ions. The latter will sputter fragments with higher molecular weights and would decrease the kinetic energy of the species bombarding the film which is growing on the substrate favoring for a mostly linear structure (high [F]/[C], and CF_2 and CF_3 moieties) and less crosslinked deposited films. Higher [F]/[C] ratios together with relatively high roughness of those coatings make them hydrophobic enough to be applied in the MD process.

The connectivity number or the possible number of network forming bonds per atom is calculated for the deposited fluorocarbon films as follows [25, 49–51]:

$$m = (4\times\%C{-}CF + 3\times\%CF + 2\times\%CF_2 + \%CF_3)\,/100 \quad (4)$$

where $\%CF_3$, $\%CF_2$ and %CF and %C−CF are the contributions of the corresponded groups to the area of the C1s XPS spectra. This parameter can be used to estimate the rigidity/flexibility of the deposited films. The values lower than 2.4 characterize an underconstrained (or undercrosslinked) flexible coating while above this value the network is overconstrained (overcrosslinked). The values of *m* for all films in the present study are quite close to 2.3. The results also show that for the films prepared at the same power, the lower connectivity number corresponds to the higher $\%CF_2$.

Table 1 Fractions of CF_x components of C1s XPS peak, [F]/[C], and connectivity number for 10 min sputtering

Power (W)	Distance (cm)	Pressure (mtorr)	CF_3 (%)	CF_2 (%)	CF (%)	C-CF (%)	C-C (%)	[F]/[C]	*m*
50	5	3.8	11.48	24.87	23.24	22.64	17.77	0.85	2.21
100	5	3.8	7.37	18.14	33.46	22.64	18.39	0.66	2.35
100	10	3.8	10	22.09	31.13	21.48	15.3	0.79	2.33
100	10	20	18.79	33.83	23.76	17.96	5.66	1.27	2.29
100	5	20	15.51	24.3	27.37	21.11	11.71	1.03	2.3

It is noticeable that since detecting fluorine emission lines in argon plasma by OES is difficult because of low sputtering rate of the PTFE target i.e. its low emission intensity compared to that of argon, neon is generally used to distinguish between the atomic and ionic lines for fluorine**.** Alternatively, information about CF_x moieties on the substrate that might imply the constituents of plasma environment have been obtained by XPS analyses in the present study. However, additional investigations and modeling can elucidate the relationship between OES spectra and compositions of CF_x groups.

The hydrophobicity of the treated membranes was evaluated by measuring the static water contact angle. The changes in static contact angles and average thickness of PTFE deposited polymer films in different power inputs are shown in Fig. 7. The average thickness is increased by raising the applied power as expected since increasing the power increases the density of active species and the mean momentum of the particles in the plasma state and thereby more fragmentation from the target to create more deposition–forming species in plasma, which contribute to the film growth enhancement. However, water contact angle of the PTFE sputtered films is increased with increasing the power up to 50 W and is not affected by further RF plasma power inputs. Increasing the power results in an increase of the concentration of CF_x fragments deposited on the surface as well as increase of the surface roughness up to 50W. For higher powers, the [F]/[C] ratio is decreased, which is traded off by increment in the roughness and leads to insignificant change in WCA.

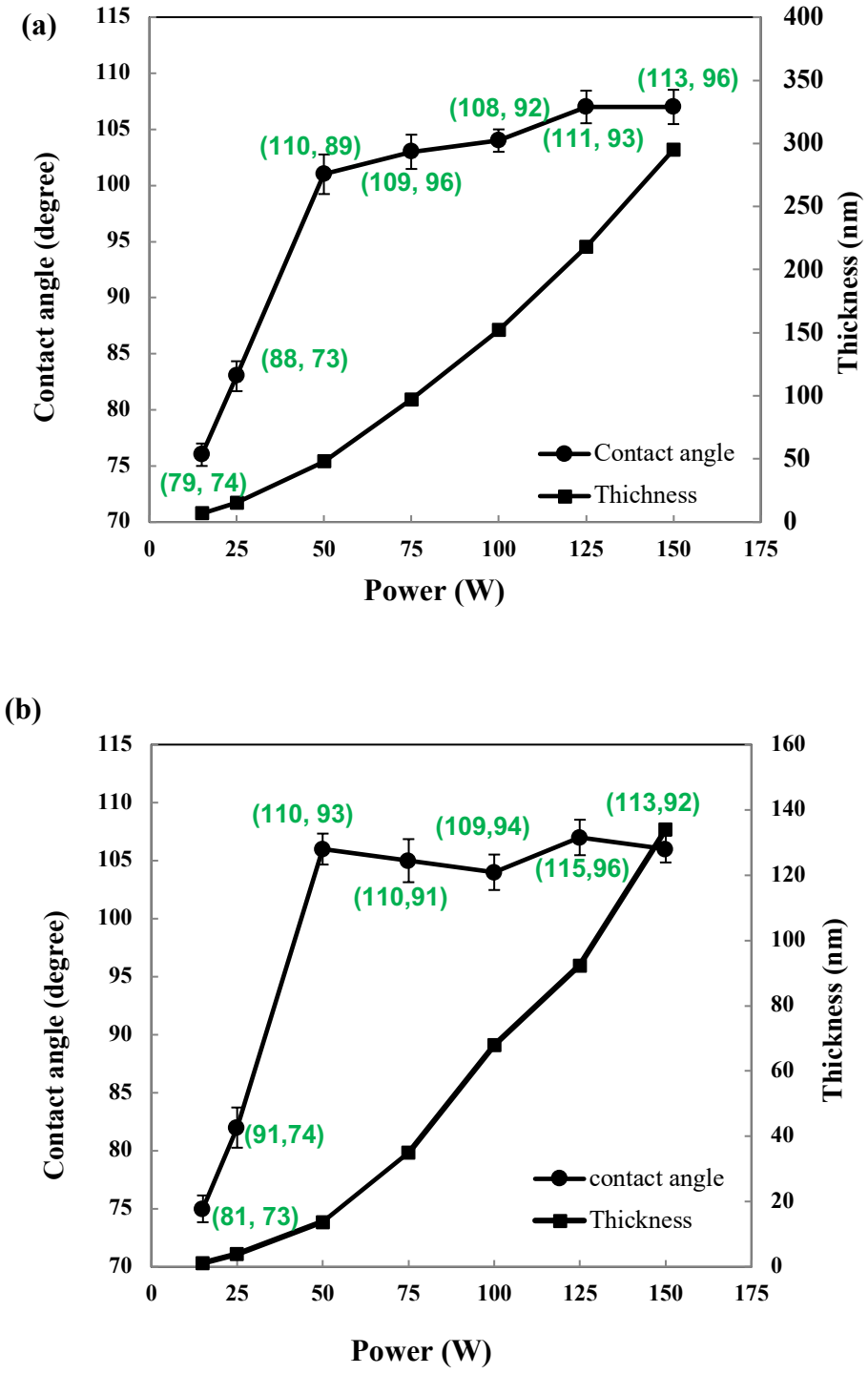

Fig. 7 Average thickness and contact angles on PTFE deposited films at different powers, p= 3.8 mTorr, Q_{Ar}= 30 sccm, 10min deposition at **(a)** 5 cm and **(b)** 10 cm target -substrate distances [the numbers in parentheses denote advancing and receding contact angles (ACA, RCA)]

Fig. 8 shows the dependence of the average thickness and WCA of PTFE deposited films to the argon pressure in the sputtering system. The WCA values are increased with increasing the argon pressure while the average thickness values show a decreasing trend with the increase in the argon pressure. At higher argon pressures, the number of collisions is increased that leads to a decrease in the mean energy of the ions. This means less fragmentation of the polymeric target and lower emission of the fragments. Moreover, at higher pressures, the mean free path of the species decreases and at a constant substrate-target distance, the reactive species, which are required for the film growth may not reach sufficiently to the substrate. Therefore, the deposition rate decreases with increasing the system pressure. The AFM analyses revealed that higher surface roughness is obtained for the polymeric films in higher working gas pressures. Therefore, the increase in WCA of the sputtered films at these pressures can be explained by the fact that the surface roughness of the films increased [52].

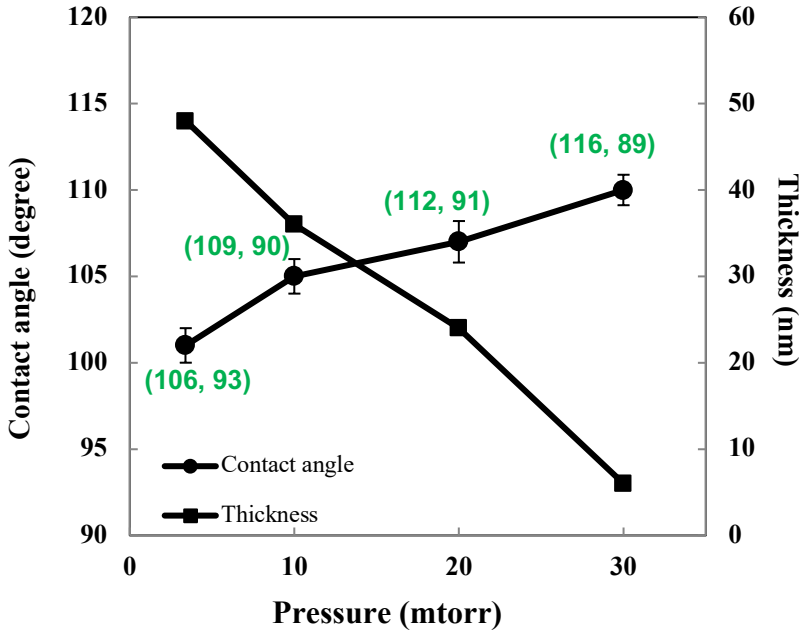

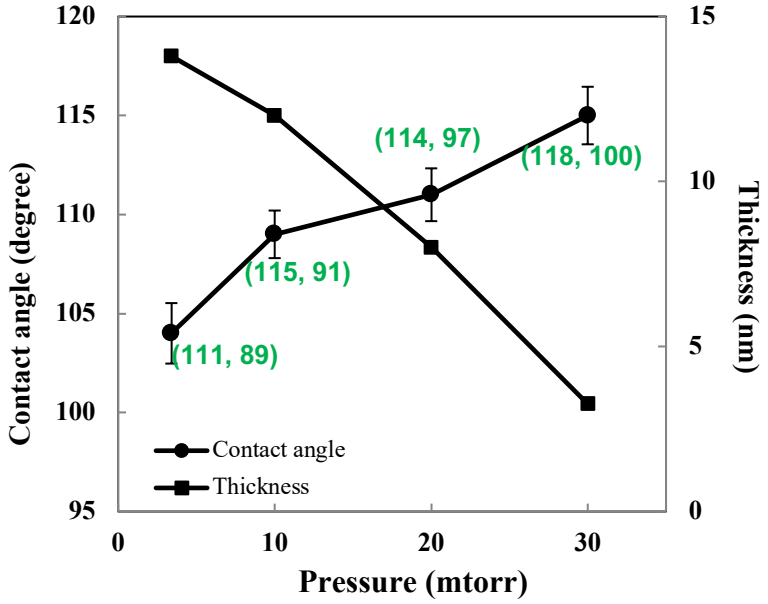

Fig. 8 Average thickness and contact angle of PTFE deposited films with different Ar pressure for power of 100W, Q_{Ar}=30 sccm, 10min deposition at **(a)** 5 cm and **(b)** 10 cm target-substrate distances (The numbers in parentheses denote advancing and receding contact angles (ACA, RCA)).

As seen in Figs. 7 and 8, the average thicknesses of PTFE sputtered films are thicker for the smaller distance. As mentioned earlier, by increasing the target-substrate distance, the density of the electrons as well as the reactive species reaching the substrate surface reduce that can explain the decrease in the deposited film thicknesses. These results are totally in agreement with those previously mentioned by Kylián et al.[25].

In order to examine the effect of aging process, the contact angles of treated membranes stored under air atmosphere in room temperature for 8 months were again tested. It was found that the contact angles of the membranes changes within 1-5%, which shows that the membranes retain their hydrophobicities and insignificant aging effect.

The surface porosities and LEPs of treated PES membranes at different treatment conditions are shown in Fig. 9. At higher RF power and lower target-substrate distances, due to the increase of the reactive species reaching to the substrate surface and lateral diffusion on the surface, the probability of surface pore clogging are increased resulting in a lower surface porosity and higher

LEP. On the other hand, increasing the total pressure in the sputtering system can increase the porosity of the deposited film without changing the average pore size in agreement with the results by Ren et al.[53] and Casari et al. [54]. The bulk porosities of all treated membranes in different sputtering conditions were determined in the range of 69-73% indicating no major changes in the membranes' bulk porosities.

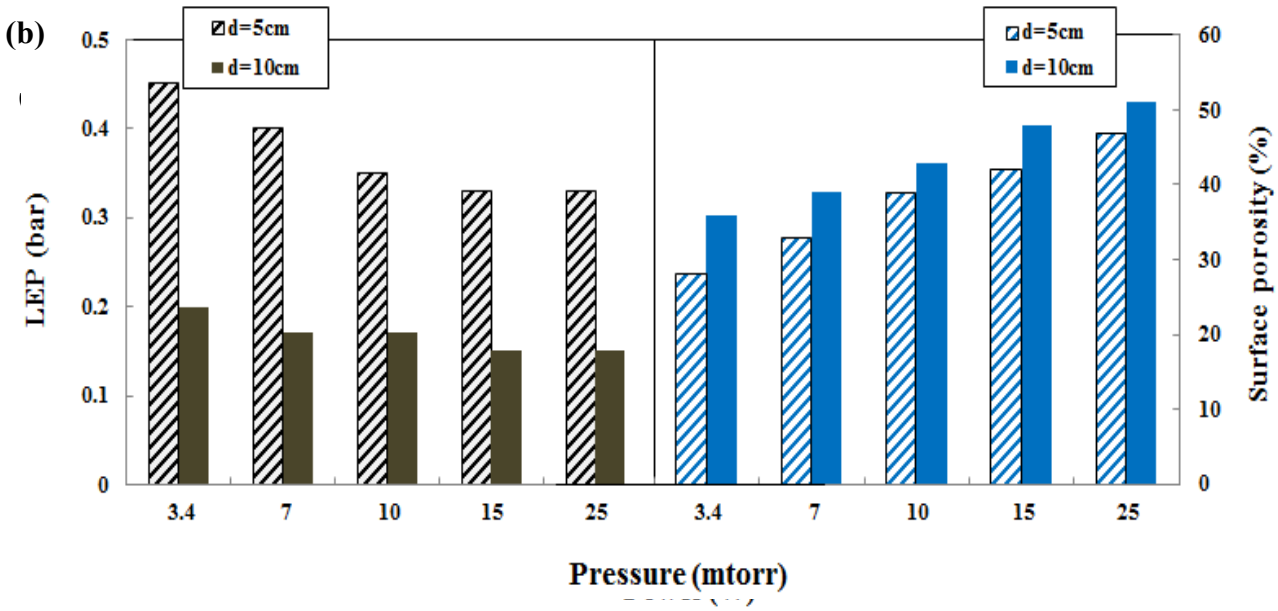

Fig. 9 Surface porosities and Liquid Entry Pressures of PTFE deposited films at two target-substrate distances against **(a)** plasma power and **(b)** argon pressure for 10 min deposition time.

3.3 AGMD performances of treated PES membranes

The performances of the treated membranes in the experimental AGMD setup were tested. The experimental parameters were set as: benzene concentration in feed solution = 300 ppm, feed temperature = 50 °C, and feed flow rate = 3ml/s. The permeate flux and separation factor of the treated membranes with changing RF power at 3.8 mtorr argon pressure, for 5 and 10 cm target-substrate distances are presented in Fig. 10. For 5 cm distance, a decrease in permeate flux is observed from 1.47 to 0.79 kg/m^2.h with raising in RF power to 100 W while the separation factor is increased up to 31, which can be contributed to the increase in the contact angle and thickness of the deposited layer as a function of power. Similar trends are observed for 10 cm distance.

It should be mentioned that the performances of modified membranes on the membrane distillation setup are usually affected by their hydrophobicity, pore size, porosity, and thickness. Although the most important characteristic of a MD membrane is its resistance against liquid entrance into the membrane pores, it does not affect significantly the vapor/liquid equilibrium of the feed solutions. In this process, the membrane is considered as a barrier (to keep?)between or to separate the vapor/liquid interfaces [1]. Increasing the contact angle by increasing applied power and pressure will help to prevent entrance of water at the interface. However, for the membrane with satisfactory hydrophobicity, the pore size and thickness of the membrane on the performance are the predominant parameters.

Considering the SEM images (Fig. 5) and AFM analysis, increasing the applied power could decrease the density and the average pore size of the pores in the deposited films. The surface porosities of the PTFE films for applied power of 50W are 28% and 36% at 5 and 10 cm substrate-target distance, respectively. These values are decreased to 18% and 28% for the membranes prepared at RF power of 100 W. In addition, at a higher power, the deposition rate is higher leading to thicker deposited layers on the membrane. The thicker layers will constitute a higher mass

transfer resistance that can explain the reduction in permeate flux through the membrane. Besides, the same reasons cause higher fluxes and lower separation factors for the treated membranes at the longer target-substrate distance.

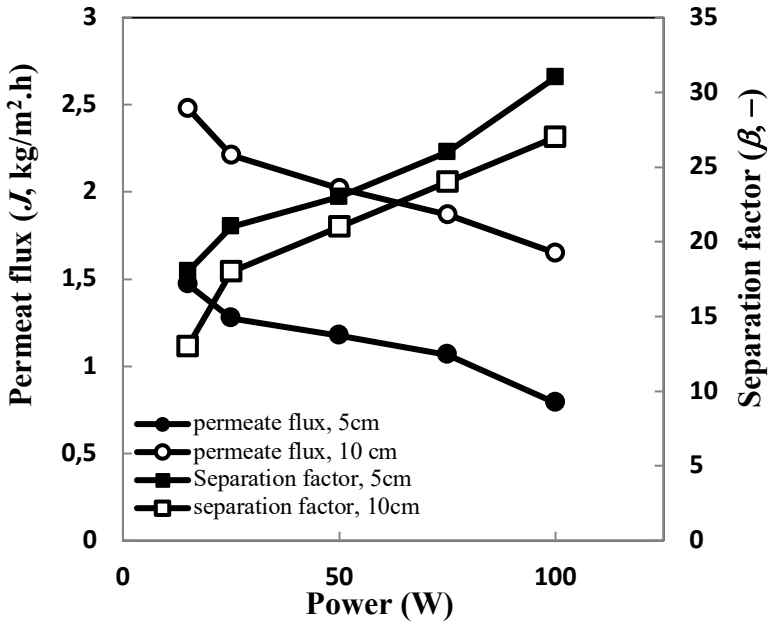

Fig. 10 Permeate fluxes and benzene separation factors against RF power for pressure of 3.8 mtorr, Q_{Ar}= 30 sccm, 10 min deposition at 5 and 10 cm target-substrate distances.

The AGMD performances of the treated membranes under different Ar pressures are also tested for 5 and 10 cm target-substrate distances as presented in Fig. 11. By increasing the Ar pressure, although a slight increase in the WCA and [F]/[C] ratio is observed, the permeate fluxes increase whereas the separation factors decrease. The increment in surface porosity by increasing the pressure helps to improve the permeate flux. Moreover, high pressure means lower deposition rate resulting in a thinner hydrophobic layer and therefore reduced mass transfer resistance across the membrane.

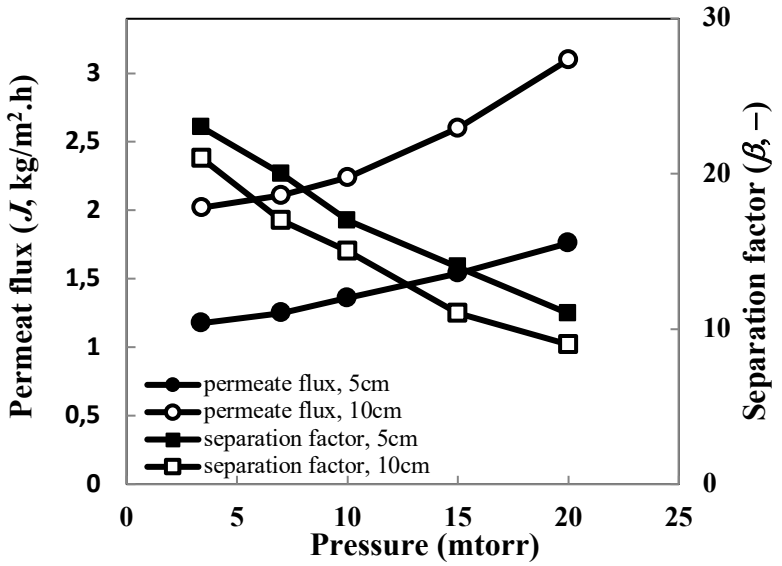

Fig. 11 Permeate fluxes and benzene separation factors against Ar pressure for RF power of 50W, Q_{Ar} = 30 sccm, 10 min deposition at 5 and 10 cm target-substrate distances.

In order to compare the AGMD performance of treated membranes with a typical PTFE commercial membrane (11806 Sartorius Stedim Biotech, pore size= 0.45μm, thickness= 80 μm, porosity= 85%), two treated membranes with the following conditions were selected: M1: 50W, 3.8 mtorr Ar pressure and 5 cm; and M2: 50W, 15 mtorr Ar pressure and 10 cm target-substrate distance. The AGMD performances of the membranes on the experimental setup in terms of removal efficiency as described below are compared in Fig. 11 within 20-h runs.

$$RE = \frac{(C_0V_0 - CV)}{C_0V_0 \times J} \tag{5}$$

where C_0 and C are the concentrations of feed and retentate, respectively, and V_0 and V are their corresponded volumes.

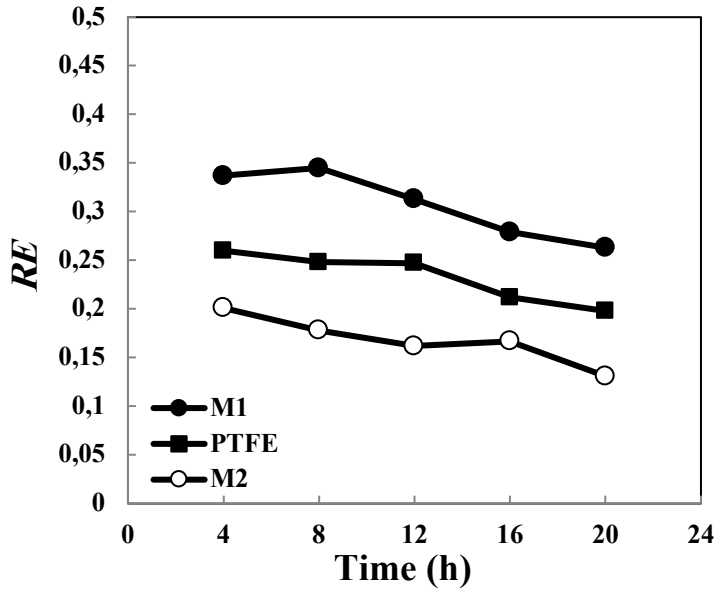

Fig. 12 Removal efficiencies of for treated PES and commercial PTFE membranes in long term runs.

As seen in the Fig. 12, all the membranes show similar trends with a slight decrease in their removal efficiencies over the time. The removal efficiencies of treated PES membrane in some treatment conditions e.g. for M1, can be superior to those of the commercial PTFE membrane.

4. Conclusion

RF magnetron sputtering of PTFE was used in the present study as a smart technique to achieve porous hydrophobic coatings on a PES substrate. The process parameters such as sputtering power, Ar pressure, and substrate-target distance were tuned to obtain different chemical structures of the deposited PTFE films. A maximum static contact angle of 115° was obtained for the PTFE-sputtered PES membranes. The XPS data indicated that the surface composition and chemical structure of the deposited films at high Ar pressure and longer substrate-target distances exhibited more resemblance to those of the PTFE film. The uniformity and hydrophobic nature of the sputter-deposited fluorocarbon polymer films enable the treated membranes to be used for the first time in an AGMD process for removal of benzene from water.

Although the sputtering power show a significant effect on the surface porosity and LEP of the treated membranes compared to the pressure, both factors strongly affect the permeation flux and separation factor in the MD process. The permeate flux increases with the increase of the argon pressure but decreases with increasing the applied RF power while a reverse trend is observed for the separation factor. It was confirmed that the hydrophobic PES membranes obtained by PTFE sputtering have comparable performances in the MD process as that of the commercial PTFE membrane for removal of benzene from a feed solution. The simple and economical fabrication procedure of PES membranes treated by PTFE sputtering as explained in the present study suggests that they can be commercially applied in the MD processes.

Acknowledgments

The authors would like to thank the Iran National Science Foundation for their financial support. The French consulate in Iran is acknowledged for awarding the mobility scholarship in France to S. Pedram.

References

1. El-Bourawi MS, Ding Z, Ma R, Khayet M (2006) A framework for better understanding membrane distillation separation process. J Memb Sci 285:4–29. doi: 10.1016/j.memsci.2006.08.002

2. Zhang Y, Peng Y, Ji S, Wang S (2016) Numerical simulation of 3D hollow- fi ber vacuum membrane distillation by computational fl uid dynamics. Chem Eng Sci 152:172–185. doi: 10.1016/j.ces.2016.05.040

3. Khayet M (2011) Membranes and theoretical modeling of membrane distillation: A review. Adv Colloid Interface Sci 164:56–88. doi: 10.1016/j.cis.2010.09.005

4. Dao TD, Mericq JP, Laborie S, Cabassud C (2013) A new method for permeability measurement of hydrophobic membranes in Vacuum Membrane Distillation process. Water Res 47:2096–2104. doi: 10.1016/j.watres.2013.01.040

5. Khayet M, Matsuura T (2011) Membrane Distillation Principles and Applications. Elsevier B.V., Oxford, UK

6. AlMarzooqi FA, Bilad MR, Arafat HA (2016) Development of PVDF membranes for membrane distillation via vapour induced crystallization. Eur Polym J 77:164–173. doi: 10.1016/j.eurpolymj.2016.01.031

7. Khayet M, Matsuura T (2001) Preparation and characterization of polyvinylidene fluoride membranes for membrane distillation. Ind Eng Chem 40:5710–5718. doi: 10.1021/ie010553y

8. Song L, Li B, Sirkar KK, Gilron JL (2007) Direct contact membrane distillation-based desalination: Novel membranes, devices, larger-scale studies, and a model. Ind Eng Chem Res 46:2307–2323. doi: 10.1021/ie0609968

9. Li B, Sirkar KK (2005) Novel membrane and device for vacuum membrane distillation-based desalination process. J Memb Sci 257:60–75. doi: 10.1016/j.memsci.2004.08.040

10. Wang H, Yang L, Zhao X, et al (2009) Improvement of Hydrophilicity and Blood Compatibility on Polyethersulfone Membrane by Blending Sulfonated Polyethersulfone. Chinese J Chem Eng 17:324–329. doi: 10.1016/S1004-9541(08)60211-6

11. Bégoin L, Rabiller-Baudry M, Chaufer B, et al (2006) Methodology of analysis of a spiral-wound module. Application to PES membrane for ultrafiltration of skimmed milk. Desalination 192:40–53. doi: 10.1016/j.desal.2005.10.010

12. Liang CY, Uchytil P, Petrychkovych R, et al (2012) A comparison on gas separation between PES (polyethersulfone)/MMT (Na-montmorillonite) and PES/TiO 2 mixed matrix membranes. Sep Purif Technol 92:57–63. doi: 10.1016/j.seppur.2012.03.016

13. Li JF, Xu ZL, Yang H, et al (2009) Effect of TiO2 nanoparticles on the surface morphology and performance of microporous PES membrane. Appl Surf Sci 255:4725–4732. doi: 10.1016/j.apsusc.2008.07.139

14. Fang HHP, Shi X (2005) Pore fouling of microfiltration membranes by activated sludge. J Memb Sci 264:161–166. doi: 10.1016/j.memsci.2005.04.029

15. Sun X (2010) Effect of the Based Membrane on the Hydrophobicity of Super-hydrophibic PES Membrane and its Structural Properties. Mod Appl Sci 4:71–77.

16. Khayet M, Matsuura T (2003) Application of surface modifying macromolecules for the preparation of membranes for membrane distillation. Desalination 158:51–56. doi: 10.1016/S0011-9164(03)00432-6

17. Kylián O, Petr M, Serov A, et al (2014) Hydrophobic and super-hydrophobic coatings based on nanoparticles overcoated by fluorocarbon plasma polymer. Vacuum 100:57–60. doi: 10.1016/j.vacuum.2013.07.014

18. Laird ED, Bose RK, Wang W, et al (2013) Carbon nanotube-directed polytetrafluoroethylene crystal growth via initiated chemical vapor deposition. Macromol Rapid Commun 34:251–256. doi: 10.1002/marc.201200678

19. Iwamori S, Hasegawa N, Uemura A (2008) Fluorocarbon polymer thin films prepared by three different types of r.f. magnetron sputtering systems. Surf Coatings Technol 203:59–64. doi: 10.1016/j.surfcoat.2008.07.035

20. Qi H, Zhang Y, Di J, Du W (2007) Morphology and structure of polymer fluorocarbon coatings on polyimide by sputtering. Mater Sci 201:5522 – 5525. doi: 10.1016/j.surfcoat.2006.07.222

21. Kwong HY, Wong MH, Wong YW, Wong KH (2007) Superhydrophobicity of polytetrafluoroethylene thin film fabricated by pulsed laser deposition. Appl Surf Sci 253:8841–8845. doi: 10.1016/j.apsusc.2007.04.036

22. Zhang Y, Yang GH, Kang ET, et al (2002) Deposition of Fluoropolymer Films on Si (100) Surfaces by Rf Magnetron Sputtering of Poly(tetrafluoroethylene). Langmuir 18:6373–6380. doi: 10.1021/la011606j

23. Morrison DT, Robertson T (1973) R.F sputterng of plastics. Thin Solid Films 15:87–101.

24. Tibbitt JM, Shen M, Bell AT (1975) A comparison of r.f. sputtered and plasma polymerized thin films of tetrafluoroethylene. Thin Solid Films 29:85–87. doi: 10.1016/0040-6090(75)90187-X

25. Kylián O, Drábik M, Polonskyi O, et al (2011) Deposition of nanostructured fluorocarbon plasma polymer films by RF magnetron sputtering of polytetrafluoroethylene. Thin Solid Films 519:6426–6431. doi: 10.1016/j.tsf.2011.04.213

26. Jafari R, Menini R, Farzaneh M (2010) Superhydrophobic and icephobic surfaces prepared by RF-sputtered polytetrafluoroethylene coatings. Appl Surf Sci 257:1540–1543. doi: 10.1016/j.apsusc.2010.08.092

27. Kim HM, Sohn S, Ahn JS (2013) Transparent and super-hydrophobic properties of PTFE films coated on glass substrate using RF-magnetron sputtering and Cat-CVD methods. Surf Coatings Technol 228:S389–S392. doi: 10.1016/j.surfcoat.2012.05.085

28. Stelmashuk V, Biederman H, Zemek J, Trchova M (2005) Plasma polymer films rf sputtered from PTFE under various argon pressures. Vaccum 77:131–137. doi: 10.1016/j.vacuum.2004.08.011

29. Drábik M, Polonskyi O, Kylián O, et al (2010) Super-hydrophobic coatings prepared by RF magnetron sputtering of PTFE. Plasma Process Polym 7:544–551. doi: 10.1002/ppap.200900164

30. Suzuki Y, Fu H, Abe Y, Kawamura M (2013) Effects of substrate temperature on structure and mechanical properties of sputter deposited fluorocarbon thin films. Vacuum 87:218–221. doi: 10.1016/j.vacuum.2012.05.029

31. Franco JA, Kentish SE, Perera JM, Stevens GW (2011) Poly(tetrafluoroethylene) sputtered polypropylene membranes for carbon dioxide separation in membrane gas absorption. Ind Eng Chem Res 50:4011–4020. doi: 10.1021/ie102019u

32. Rastegarpanah A, Mortaheb HR (2016) Surface treatment of polyethersulfone membranes for applying in desalination by direct contact membrane distillation. Desalination 377:99–107. doi: 10.1016/j.desal.2015.09.008

33. Ma J, Ashfold MNR, Mankelevich YA (2009) Validating optical emission spectroscopy as a diagnostic of microwave activated CH4 /Ar/ H2 plasmas used for diamond chemical vapor deposition. J Appl Phys 105:1–12. doi: 10.1063/1.3078032

34. Rácz G, Kerker S, Kovács Z, et al (2014) Theoretical and Experimental Approaches of Liquid Entry Pressure Determination in Membrane Distillation Processes. Period Polytech Chem Eng 58:81–91. doi: 10.3311/PPch.2179

35. Khayet M, Khulbe K, Matsuura T (2004) Characterization of membranes for membrane distillation by atomic force microscopy and estimation of their water vapor transfer coefficients in vacuum membrane distillation process. J Memb Sci 238:199–211. doi: 10.1016/j.memsci.2004.03.036

36. Wu YJ, Huang QL, Xiao CF, et al (2014) Study on the effects and properties of PVDF/FEP blend porous membrane. Desalination 353:118–124. doi: DOI 10.1016/j.desal.2014.09.010

37. Vandencasteele N, Nisol B, Viville P, et al (2008) Plasma-modified PTFE for biological applications: Correlation between protein-resistant properties and surface characteristics. Plasma Process Polym 5:661–671. doi: 10.1002/ppap.200700143

38. Canal C, Gaboriau F, Villeger S, et al (2009) Studies on antibacterial dressings obtained by fluorinated post-discharge plasma. Int J Pharm 367:155–161. doi: 10.1016/j.ijpharm.2008.09.038

39. Prathyusha1 T, Reddy CS, Reddy PS, Reddy AS (2014) Effect of sputtering power on the physical properties of dc magnetron sputtered copper oxide thin films. Int J ChemTech Res 6:3349–3352. doi: 10.1016/j.matchemphys.2008.02.031

40. Baker MA, Fakhouri H, Grilli R, et al (2014) Effect of total gas pressure and O2/N2 flow rate on the nanostructure of N-doped TiO2 thin films deposited by reactive sputtering. Thin Solid Films 552:10–17. doi: 10.1016/j.tsf.2013.11.111

41. Zhang Y, Yang GH, Kang ET, et al (2002) Characterization of fluoropolymer films deposited by magnetron sputtering of poly(tetrafluoroethylene) and plasma polymerization of heptadecafluoro-1-decene (HDFD) on (100)-oriented single-crystal silicon substrates. Surf Interface Anal 34:10–18. doi: 10.1002/sia.1243

42. Srinivas K, Manivel Raja M, Sridhara Rao D V., Kamat S V. (2014) Effect of sputtering pressure and power on composition, surface roughness, microstructure and magnetic properties of as-deposited Co2FeSi thin films. Thin Solid Films 558:349–355. doi: 10.1016/j.tsf.2014.02.052

43. Stelmashuk V, Biederman H, Slavínská D, et al (2005) Plasma polymer films rf sputtered from PTFE under various argon pressures. Vacuum 77:131–137. doi: 10.1016/j.vacuum.2004.08.011

44. Chawla V, Jayaganthan R, Chawla AK, Chandra R (2008) Microstructural characterizations of magnetron sputtered Ti films on glass substrate. J Mater Process Technol 9:3444–3451. doi: 10.1016/j.jmatprotec.2008.08.004

45. Golub MA, Wydeven T, Johnson AL (1998) Similarity of Plasma-Polymerized Tetrafluoroethylene and Fluoropolymer Films Deposited by rf Sputtering of Poly(tetrafluoroethylene). Langmuir 14:2217–2220.

46. Bayat A, Ebrahimi M, Nourmohammadi A, Moshfegh AZ (2015) Wettability properties of PTFE/ZnO nanorods thin film exhibiting UV-resilient superhydrophobicity. Appl Surf Sci 341:92–99. doi: 10.1016/j.apsusc.2015.02.197

47. Becker C, Petersen J, Mertz G, et al (2011) High superhydrophobicity achieved on poly(ethylene terephthalate) by innovative laser-assisted magnetron sputtering. J Phys Chem C 115:10675–10681. doi: 10.1021/jp200517e

48. Jafari R, Momen G, Farzaneh M (2016) Durability enhancement of icephobic fluoropolymer film. J Coatings Technol Res 13:405–412. doi: 10.1007/s11998-015-9759-z

49. Döhler GH, Dandoloff R, Bilz H (1980) A topological-dynamical model of amorphycity. J Non Cryst Solids 42:87–95. doi: 10.1016/0022-3093(80)90010-1

50. Winder EJ, Gleason KK (2000) Growth and characterization of fluorocarbon thin films grown from trifluoromethane (CHF3) using pulsed-plasma enhanced CVD. J Appl Polym Sci 78:842–849. doi: 10.1002/1097-4628(20001024)78:4<842::AID-APP180>3.0.CO;2-J

51. Limb SJ, Gleason KK, Edell DJ, Gleason EF (1997) Flexible fluorocarbon wire coatings by pulsed plasma enhanced chemical vapor deposition. J Vac Sci Technol A 15:1814–1818. doi: 10.1116/1.580796

52. Roach P, Shirtcliffe NJ, Newton MI (2011) Mimicking natural superhydrophobic surfaces and grasping the wetting process: a review on recent progress in preparing superhydrophobic surfaces. Adv Colloid Interface Sci 169:80–105. doi: 10.1016/j.cis.2011.08.005

53. Ding R, Yu Z, ChangYong Z, NingKang H (2011) Study on the Porosity of TiO2 Films Prepared by Using Magnetron Sputtering Deposition. J Korean Phys Soc 58:883–885. doi: 10.3938/jkps.58.883

54. Casari CS, Giannuzzi CS, Russo V (2016) Carbon-atom wires produced by nanosecond pulsed laser deposition in a background gas. Carbon N Y 104:1–15. doi: 10.1016/j.carbon.2016.03.056